Chracterization of LabVIEW based 16-electrode 2D EIT system

Nanda V. Ranade[1], Damayanti C. Gharpure [2]

Department of Electronic Science, Savitribai Phule Pune University, India

Abstract: *Characterization of EIT system is crucial for validation and calibration. Parameters used for characterization are divided into two groups- first dealing with data quality (SNR, accuracy) and second dealing with image quality (CNR, RNG, reconstructed area).These parameters are useful while selecting a particular EIT system for any new application. Injected current directly affects the data and hence the quality of reconstructed image. Therefore we have studied effect of amplitude of injected current on the EIT data and reconstructed image experimentally. Guidelines are evolved for setting the EIT system to collect useful data for further characterization. We report a set of experiments carried out to characterize a Lab VIEW based 16-electrode 2D EIT system developed in our laboratory. SNR and accuracy for all 208 channels involved in the Sheffield measurement pattern has been calculated. Resolution of EIT system is an important parameter and it depends on both data and image quality and is a combined index for the performance. Uniformity of resolution over the object is also important to preserve shape characteristics of target. We have obtained the resolution of our system experimentally at the centre as well as near the electrodes. It is shown to follow the limits proposed by Seagar relating to the model used for reconstruction and by Isaacson relating to the noise in the measurement.*

Keywords: *EIT, Data Quality, Image Quality,Evaluation, Resolution*

I. Introduction

Electrical Impedance Tomography gives conductivity images of an object by injecting current in it and measuring voltages developed on its surface [1]. Since its introduction around three decades ago, it is recognized as a non invasive and less costly technique to probe internal nature of an object [2]. It is mainly used in medical imaging and process tomography. Recently several other applications in Non Destructive Testing (NDT) are being explored. The interest in this area is increasing and several research laboratories have built their own EIT systems using different technologies. The hardware required to build an EIT system with moderate specifications is not very complicated. At the same time open source software for reconstruction- EIDORS [3] is available. As a result of this many groups have reported their EIT systems along with reconstructed images of targets such as plastic rods, metal rods or clay [4][5][6]. In order to evaluate the system we need to systematically judge various parameters which act as performance indicators. EIT reconstruction is an ill posed problem and it is sensitive to the variation in data. A small variation in data may lead to an altogether different image [7]. Even with a system having good performance index, it is possible to acquire a data which leads to wrong reconstruction. Maimaitijiang et al [8] have described a systematic approach to evaluate performance of EIT system using different parameters which act as performance indicators. They classify the parameters as data quality (Signal to Noise Ratio-SNR, accuracy, drift, and reciprocity), detectability, and image quality (amplitude response, position error, resolution, ringing). A few of these parameters are used by some groups to characterize their systems [9]. Bera et al [4] use contrast to noise ratio (CNR) to analyze the quality of the reconstructed image. In this light, effect of injected current on reconstructed images has been studied. Analyzing the acquired data for different injected currents, we propose a guideline to be followed while acquiring EIT data. The evaluation parameters have been obtained, with the data collected following the guidelines.

In this work we report characterization of the 16-electrode 2D EIT system developed in our laboratory [10]. We have measured the SNR, accuracy, CNR, ringing, reconstructed area and resolution as the parameters to characterize our system.The rationale behind using these parameters is explained in section II. We have carried out experiments, analyzed the data and reported these parameters in standard formats. EIT is placed at lower rank compared to other tomography techniques due to its resolution. Resolution of EIT system depends on both data and image quality. Isaacson [11] has related it to the uncertainty or noise in the measurement and Seagar [12] has related it to the reconstruction model. In this work we have determined the value of resolution for our system using two experimental techniques. It is found that these values tally well with each other and also with the limits stated by Isaacson and Seagar.

II. Materials and methods

2.1 Configuration of the EIT system and data acquisition VI

The developed EIT system (Fig.1) consists of 18 cm diameter cylindrical tank fitted with 16 steel electrodes of 1cm^2 area each along a single plane.
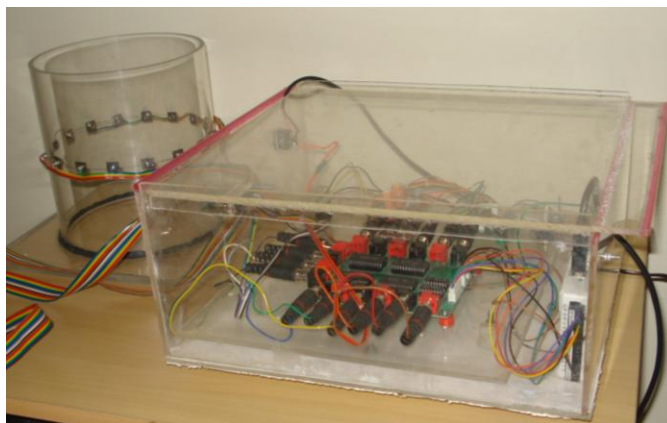
Figure 1. EIT system used for characterization

The electrodes are interfaced with the electronics using a flat cable and a 25-pin D-type connector. The circuit is in the form of two PCBs, one for multiplexers with a differential amplifier and other for variable amplitude current source. Lab VIEW based software controls the selection of electrodes through multiplexers. The same software also acquires the differential voltage using USB6009 data acquisition card. Sheffield protocol is used for data collection. This involves exciting adjacent electrodes and making adjacent measurements excluding the excitation electrodes. Total number of differential voltages also called as channels that make one frame of data is hence 16*13 equal to 208. The software is capable of taking desired number of frames one after the other automatically or as per user's choice. The frequency of excitation is 2 KHz and the sampling rate is 20 K per second. The software stores all samples of a particular channel along with the minimum and maximum value for that channel. Fig.2(a) shows the block diagram of the VI for control, sampling and acquisition of data.

Inset: portion of screen 2 showing the plot
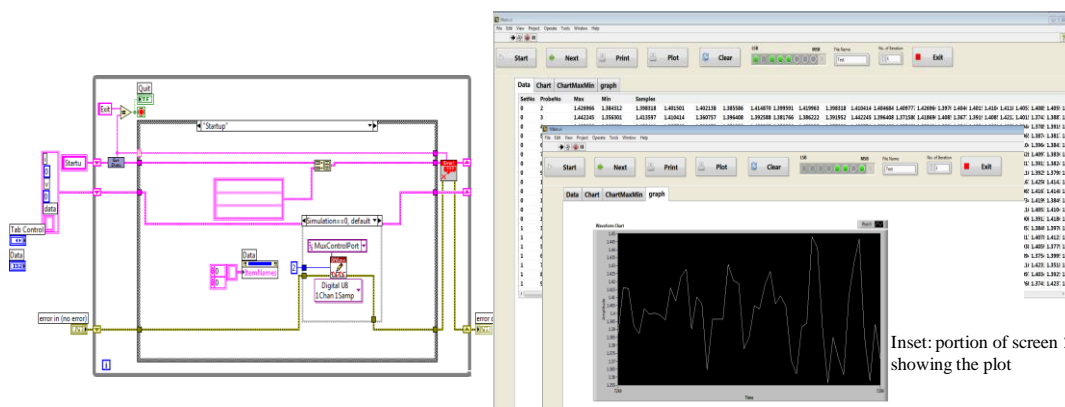
Figure 2. (a) Block diagram for Data acquisition VI (b) Screen shot of GUI used for data acquisition

The procedure for data acquisition is as follows. The vessel is cleaned with a muslin cloth. The electrode surface is cleaned, rubbed and it is ensured that it doesn't have any traces of salt from previous experiments. Vessel is then filled with 5 Liters of filtered drinking water and salt is added to set the conductivity as per requirement. The conductivity is measured using HANNA HI8733 model of conductivity meter. When the solution is still, electronic circuits are powered on and Lab VIEW VI is executed. Fig.2 (b) shows the screen shot of the data acquisition GUI. User can set the number of data frames to be acquired by entering a number in 'No of Iterations'. The EXCEL file name to which the data is saved at the end of acquisition can also be set. A click on 'Start' button starts the acquisition. Address appearing on Port0 of the USB6009 appears as a visual indication at 'MSB—LSB' location. 'Set No' corresponds to particular current excitation pair. 'Probe No' indicates specific differential voltage. The sampled voltages appear in the cells along the same row as that of 'Probe No'. The maximum and minimum voltage samples for a specific differential voltage are displayed just next to the 'Probe No'. The data can be 'Cleared' and new acquisition can start. A graph of real time voltage is shown if we click on 'Graph' button instead of 'Data'. This facility gives a visual indication, which helps to quickly check whether the acquired data is as per expectation while setting up or testing the system. The acquisition stops after set number of frames are acquired and data is stored in the file name set by the user. The data is then analyzed using EXCEL and also copied in a tab-delimited '.txt' file for reconstruction. The peak-to-

peak amplitude of each channel is used for reconstruction. EIDORS3.5 is used for 2D reconstruction. The procedure for collecting data with different targets is exactly same. Targets used were metal or plastic rods with length 20 cm, same as the height of vessel and either suspended or placed vertically at the base in the vessel filled with salt solution.

2.2 Factors influencing data and image quality
The inverse problem of reconstruction in EIT is ill posed and hence very sensitive to the data. The image quality depends on both data as well as the reconstruction algorithm. Therefore one needs to carefully understand various factors influencing the quality of data and image. There are several variables in the system, which directly or indirectly affect the image. Increase in vessel size increases the distance between the electrodes. The resolution of the system is approximately half of the distance between two electrodes [12]. Therefore increasing vessel size decreases the resolution. Other effect is increase in size increases all voltage measurements because more resistance is offered for the same current excitation. This may increase the SNR resulting in better image quality. Also increase in number of electrodes deceases distance between electrodes and hence increases resolution. But when distance between two electrodes decreases, the signal amplitude is smaller which decreases the SNR. The cabling used to connect the electronics, the type of electrodes used [13,6,14,15] and the excitation frequency affect the SNR and image quality. Injected current directly affects the data and therefore the reconstructed image. Increase in amplitude of current increases amplitude of measured signal. Assuming that noise remains the same, this should increase the SNR and hence the quality of reconstructed image. In our case size of the vessel is taken to be 18 cm in diameter and number of electrodes 16 with excitation frequency fixed as 2 KHz. Therefore initially experiments were carried out to optimize the amplitude of injected current to obtain a good image. The homogeneous data at different current values is studied to obtain the optimum value of current. This whole exercise results in some simple but important guideline for setting the system before collecting data either with or without target as discussed in the next sections.

2.3 Performance evaluation parameters
As discussed before performance parameters are mainly categorized into two types; related to data and related to image. Parameters related to data entirely depend on the hardware; whereas parameters related to image depend on hardware as well as reconstruction software. The parameters related to data are mostly obtained using data acquired on homogeneous conductivity distribution. Parameters related to image are based on reconstructed images of targets. The following parameters have been considered for characterization of the EIT system.

2.3.1 SNR
The reconstructed image of internal conductivity distribution is very sensitive to small variations in the data collected from the surface of the object. Therefore the quality of data is of immense importance and the S/N ratio decides the precision of measurement. It is easy to calculate the S/N ratio based on several frames collected on homogeneous conductivity distribution and is defined as follows-

$$SNR_i = \frac{[\bar{v}]_i}{SD_{[v]_i}} \qquad (1)$$

Here 'i' indicates the channel number. Channel number represents a particular differential voltage in the EIT data. The adjacent excitation and adjacent measurement protocol (Sheffield protocol) used in the system has 208 such channels. SNR for a particular channel is the ratio of average voltage for several measurements on that channel and their standard deviation. Percentage variability is calculated using standard deviation for every channel and 'x' the maximum variability decides the detection limit.

2.3.2 Accuracy
Accuracy is the closeness with which measurement represents the true value. It has a direct role in deciding image characteristics. In case of EIT data we take the true value as the one we obtain by simulation. Accuracy is defined for 'i'[th] channel as follows

$$AC_i = \left(1 - \left|[\bar{v}]_i - [v^{sim}]_i\right|\right) \times 100\% \qquad (2)$$

We solve the forward problem for our system and find the simulated electrode voltages v[sim] for every channel 'i'. Since we claim that it is the true value, we need to ensure that there is least possible numerical error while solving the forward problem.

The size of finite elements used to discretize the forward problem plays a major role in deciding the numerical error. A fine mesh with smaller individual finite elements causes smaller numerical error. But at the same time requires more time and memory for solving the problem. Therefore we need to carefully decide the size of finite elements. In case of our system we start with very fine mesh containing 6400 elements and solve

the forward problem. The 'meas' field of forward solution contains the simulated differential voltages. These are saved in an Excel sheet. Then we start simulating with coarse mesh containing 256, 576, 1024 and 1600 elements. These element values are decided by number of rings we choose in the forward model of the vessel. The simulated voltages for these meshes are also saved in the same Excel sheet. The relative error in simulated voltages with respect to the fine mesh solution is calculated for each mesh. Suppose 'x' is the maximum variability, then we choose the mesh that provides relative error well below 'x'.

2.3.3 Resolution

Resolution refers to size of the smallest object that could be detected by EIT system. Determination of resolution is also important since a uniform resolution causes less shape distortion in a reconstructed image [19]. Seagar et al [12] discuss the theoretical limits for resolution. If we have 'N' number of independent measurements, we can find 'N' number of unknown conductivities. That means we can have those many finite elements having different conductivities in the mesh. The size of each element gives the resolution of the system. System with 16 electrodes and Sheffield protocol has 208 measurements in a frame, out of which 104 are independent. Seagar et al show that the element size is approximately equal to half of the distance between two electrodes. This is theoretically found limit on the smallest detectable size. Isaacson [11] discusses the same problem in the name of distinguishability. He derives an expression for radius of smallest detectable object considering presence of noise as follows-

$$R_m = [\varepsilon(\varepsilon + 2)]^{1/2} \qquad (3)$$

R_m gives minimum radius of the object detectable using measurements with precision equal to ε. Apart from these theoretical derivations, there are experimental methods to find resolution of EIT system [20]. They mainly consist of finding response of EIT system to point disturbance which is called point spread function (PSF). Simulation studies of Wheeler consist of taking a single element having 2% conductivity difference from background. Reconstruction of this point disturbance comes out to be a circular region which is the PSF. Area of this region is found out using 'Full Width Half Maximum' (FWHM) method. Square root of the ratio of area of PSF to that of background is the resolution. Adler [19] defines this as the 'Blur Radius' (BR). We have used two methods to decide resolution of our system. In the first method we start from a bigger object; place it at the center; acquire data and reconstruct its image. Then go on reducing the diameter and repeat the same procedure till reconstructed image resembles the object. Radius of smallest object decides resolution of the system at the center. The second method is based on placing a point disturbance at the position where one wants to find the resolution. We have used plastic rods of different cross sections as targets for the first method. For the second method we used a brass rod with diameter equal to 5 mm. The ratio of cross sectional area of vessel and area of rod is 1296. This means the metal rod can represent a point change in the background conductivity. We follow Adler's definition for Blur Radius and represent the resolution as follows where Aq is the reconstructed target area and Ao is the total area.

$$BR = \sqrt{\frac{A_q}{A_o}} \qquad (4)$$

2.3.4 Image quality

The quality of reconstructed image depends on the quality of data as well as the reconstruction algorithm. We use inverse solver by Andy Adler based on Adler and Guardo[19]. It has one-step Gauss Newton linear difference algorithm. The prior used is NOSER prior with NOSER exponent set to 0.55.
The quality of the image is assessed using Contrast to Noise Ratio (CNR) [4], Ringing (RNG) [8] and the actual reconstructed area. CNR involves ratio of difference between target and background conductivity to the weighted noise. We decide CNR for reconstructed images of targets. CNR (contrast to noise ratio) is defined as follows-

$$CNR = \frac{BC_{mean} - IC_{mean}}{\sqrt{(W_I SD_{IC}^2 + W_B SD_{BC}^2)}} \qquad (5)$$

Where IC_{mean} and BC_{mean} are mean conductivities of target and background, SD_{IC} an SD_{BC} are standard deviations and W_I and W_B are fraction of total area for target and background respectively in the reconstructed image. The Region Of Interest (ROI) used, while calculating the area is defined as half of the maximum value. CNR is similar to the detectability used by Maimaitijiang et al[8]. Detectability is the measure of system to detect a target on certain noise background where noise is represented as standard deviation. But the formula for CNR considers noise for target and background as separate with individual weight. Therefore it provides better representation of image quality than detectability [16].The second important image quality is ringing effect. It is the measure of ringing present in the radial profile of the reconstructed image. Ringing is demonstrated as region of opposite conductivity surrounding the target. It is defined as follows.
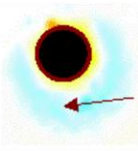
(http://eidors3d.sourceforge.net/tutorial/GREIT-evaluation)
A_{out} is the area having opposite conductivity to that of target outside the circle with its center at Center of Gravity (CG) of target and A_{in} is the area of target in the reconstructed image. The ROI used while calculating the area is defined as half of the maximum value. We calculate reconstructed target area and compare it with actual cross sectional area of the target. This is useful in 2D imaging.The reconstructed area of target is calculated as fraction of total area and then the actual area is found by multiplying it with cross sectional area of tank.

III. Experimentation and resutls

3.1 Optimization of injected current

We have studied the effect of amplitude of injected current on the reconstructed image in order to optimize its value. The conductivity of background solution is kept at 0.05 S/m. Plastic bottle with radius equal to 3.5 cm is used as a target. It is placed at three different locations; at the center, half way from center and at periphery near electrode 11. The current is varied from 0.5mA to 1.5 mA in steps of 0.1 mA. The experiment is also carried out with increased conductivity 0.1 S/m and increased current. Reconstructed images are visually analyzed to decide the optimum current. Fig.3 shows the reconstructed images for six different currents (row wise) with the target at 3 different positions (column wise).The 'maximum' and 'minimum' of EIDORS color-bar is given for each reconstructed image separately. It is observed that for any value of current as we move the object from center towards periphery, the contrast increases. When current is 0.5 mA, the central target is not reconstructed to its true shape. Similarly the other two target positions and shapes are distorted. When current is increased to 0.6 mA, central target is reconstructed to its true shape but other two positions are still with the same distortion. The contrast is better for the position at the periphery. For current equal to 0.7 mA, the contrast is still better and the shape of peripheral position is improved. Current of 0.8 mA increases the contrast further and is able to differentiate between the positions. At 0.9 mA we get the highest contrast. At current of 1 mA images of targets are nearly same but contrast is less. Therefore we can infer that 0.9 mA of current is most appropriate for this experimental arrangement. Experiments are also carried out for higher values of currents up to 1.5 mA. They do not result in reconstructions truthful to the target positions and shapes. This means that for every experimental arrangement there is some optimum value of current that should be used to probe the targets. The observations on homogeneous data acquired without placing targets, gives us some insight on deciding what is an optimum current for a specific experimental arrangement. Fig.4 shows the plots for homogeneous data taken at current values equal to 0.5 mA, 0.9 mA and 1.5mA. It is observed that as the current increases, the peak value for acquired voltage goes on increasing. The voltage crosses 5 Volt, which is the upper limit on signal amplitude when the current is 1.5 mA. In other words the signal saturates when current is 1.5 mA. Similarly the bottom portion of 'U' shape data is distorted to a large extent for current equal to 1.5 mA. We can reason out the observed tendencies in the reconstructed images on the basis of these facts. At very low current, the acquired data does not have sufficient SNR to give good quality image. At very high current, the acquired data loses some information due to saturation resulting in bad image. At currents which give homogeneous data approximately 75% of the maximum allowed signal voltage (approximately 3.5 to 4 Volt for our system), the SNR is sufficient to produce good images, without losing any details. Non conducting target may increase the voltage for some channels, but the 25 % margin does not allow the voltage to go beyond allowed limit.
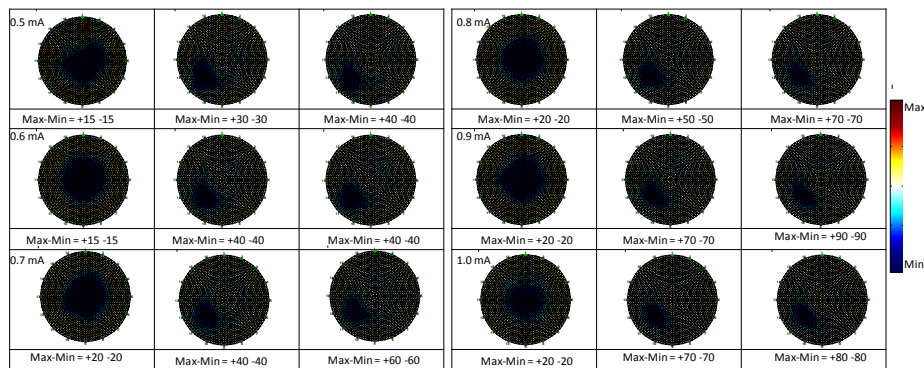
Figure3. Reconstructions at 6 different currents with target at 3 positions
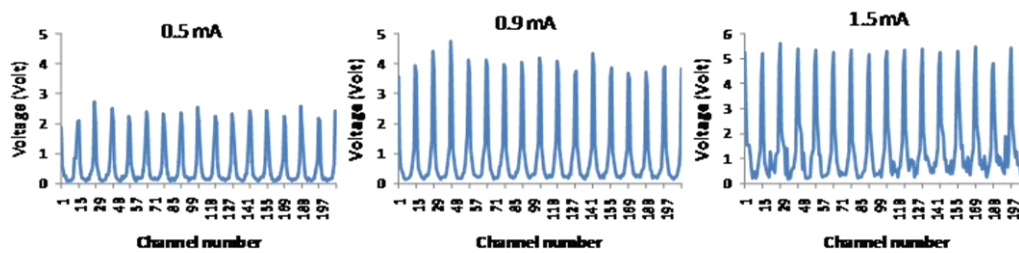
Figure 4. Homogeneous data for different current values

In the experimental arrangement we have fixed conductivity equal to 0.05 S/m. The current amplitude of 0.9 mA gives a homogeneous data with amplitude that exactly satisfies the requirement stated above and therefore it produces best images for this arrangement. In order to cross verify this argument, the experiment is repeated with conductivity of background changed to 0.1 S/m. According to the reasoning given previously, we should find that increased current satisfies the requirements regarding acquired data. Fig.5(a) shows the homogeneous data acquired at 2 mA. The maximum voltage is around 3.5 Volt which is around 75% of maximum allowed voltage. Therefore we expect good quality from reconstructed image for this background. The same bottle in previous experiment is used and it is placed near electrode 11. Fig.5(b) shows the reconstructed image. The target is shown with a good contrast at right location.
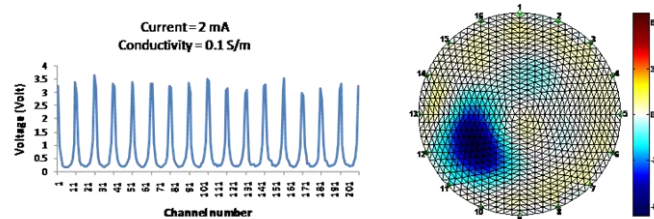
Figure 5 (a) Homogeneous data and (b) Image of target near electrode 11

We make some useful recommendation based on these experiments. Differential reconstruction makes use of two data sets one called homogeneous data acquired without placing any target and the other data set acquired by placing targets at specific position. Quality of the reconstructed image depends on both the data sets. But as seen from the experiments earlier, good quality of image can be ensured based on characteristics of homogeneous data. The maximum range of homogeneous data depends on several factors in the experimental arrangement like number and typeof electrodes, vessel geometry, conductivity of background, amplitude of excitation current and gain of amplifier. The experiments carried out during current optimization indicate that by controlling any of the above mentioned variables, setting the peak of homogeneous data to around 75% of maximum range results in good quality reconstructed images.

3.2 Characterization of the EIT system
3.2.1 Measurement of SNR and Accuracy

The SNR analysis is carried out for homogeneous conductivity distribution for two different conductivity values of salt solution 0.044 S/m and 0.06 S/m.We acquired thirty consecutive frames of data, transferred the data in EXCEL sheet and calculated SNR for each channel using the 'Average' and 'Stdevp' functions in EXCEL. The plot of SNR for all 208 channels uses the sequence of channels proposed by Gagnon et al [17]. It is easy to visually pinpoint any flaw using this sequence. In this scheme, channels are not grouped according to excitation but according to their relative position with respected to the excitation electrodes. For example 16 channels immediately next to every excitation electrode, are taken first (ie. voltage between 3-4 for excitation between1-2, voltage between 4-5 for excitation between 2-3 and so on). All these voltages are nearly equal. After this is the group of second channels with respect to the excitation electrode. On similar lines there are 13 groups. These groups follow an average 'U' shape for a homogeneous data. Any deviation from average 'U' shape indicates that there is some problem in acquisition. We have found the SNR for two different conductivity values of salt solution by keeping everything else same as well as the detection limit based on the percentage variability. Fig.6 shows the SNR plot for both conductivity values.
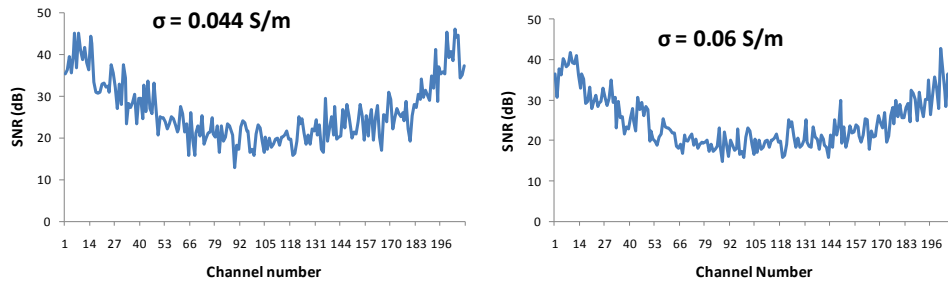
Figure 6. SNR plot for two different conductivity values

The minimum SNR is around 15 dB whereas the maximum SNR is around 45 dB. The curve follows overall 'U' shape. This means noise for all channels is nearly same. The channels near to the excitation, having more amplitude of signal show more SNR. The channels opposite to the excitation have lowest value of signal, hence show lowest SNR. Further, for higher conductivity the maximum value for SNR drops. This seems logical as higher conductivity offers lower potential for same current. Therefore signal amplitude and hence SNR decreases. The SNR analysis shows 1 % variability in the measured voltages. This helps in deciding the mesh used while solving forward problem for finding accuracy. It means that if the relative error for a selected mesh with respect to dense mesh goes well below 1%, one may decide corresponding mesh as the one to be used for accuracy calculations. Fig.7(a) shows the plot of relative error versus number of elements for meshes having different number of finite elements. The mesh with 1024 finite elements gives relative error equal to 0.4% which is well below 1%. We therefore choose a mesh with 1024 elements. This corresponds to 16 mesh rings in the forward model. The simulated voltages are then scaled with an appropriate scale factor and compared with the experimentally measured voltages used for SNR analysis to decide accuracy of every channel. Fig.7(b) shows the plot for accuracy of all 208 channels as per formula. Order of the channels is taken the same as that for SNR plot. It is observed that accuracy drops considerably for channels second next to the excitation electrodes. The reason for this is not yet clear to us and it needs to be explored.
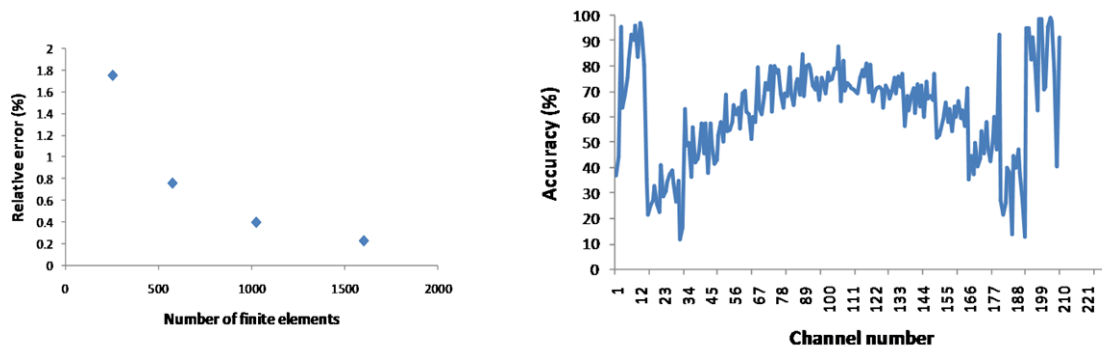
Figure 7. (a) Relative error as a function of number of finite elements (b) Plot for accuracy of 208 channels

3.2.2 Resolution
In the first method to find resolution we have taken plastic rods of radii equal to 4.6, 2.1, 1.75 and 1.35 cm. We place them at the center to find the resolution at the center. Fig.8 shows the reconstructed images.Visual inspection clearly implies that object with radius less than 2.1 cm are reconstructed either with other artifacts or are not detected at all. Therefore we can conclude that experimentally observed resolution of our system is equal to the ratio 2.1 cm/ 9 cm that is 0.23 at the center. We consider Isaacson's expression for normalized radius of smallest object which could be detected considering presence of noise. The SNR analysis shows average deviation equal to 0.04. If we substitute this value for precision (ε) in the equation, it gives R_m equal to 0.28. This is quite close to the experimentally observed value of 0.23. Thus the theoretically calculated value of minimum size detected at the center is 2.52 cm whereas experimentally found value is 2.1 cm.
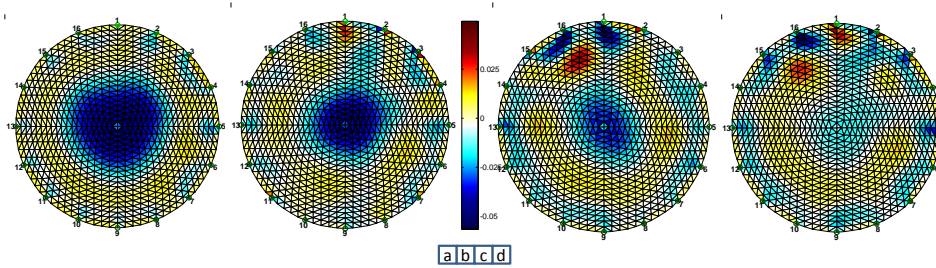
Figure 8. Reconstructions for centrally placed plastic rod with radius a) 4.6 cm b) 2.1 cm c) 1.75 d) 1.35 cm

Fig.9 shows the model for placement of metal rod and its reconstruction from experimental data which is required for second method (PSF) of determining resolution. In this method it was necessary to take the position of disturbance near periphery as the central disturbance was not detected due to noise. A point disturbance in the form of metal rod is introduced near electrodes10-11. The reconstructed image shows the increase in conductivity near the position of the rod which can be considered as point spread function of EIT system. The blur radius is calculated from the ratio of area of reconstructed target to the total area as
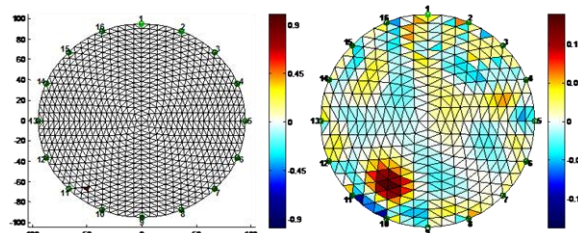
Figure 9. Model for placement of metal rod and the reconstruction of experimental data

$$BR = \sqrt{\frac{A_q}{A_o}} = 0.16$$

This means near periphery the resolution is 0.16. In other words the minimum detectable object near periphery has radius equal to 0.16*9 cm (1.44 cm) since radius of vessel is 9 cm. This value is less than that at the center. It is consistent with the finding of Wheeler [20] that resolution for adjacent excitation and adjacent measurement protocol has better value at the periphery than at the center. Table 1 summarizes the theoretical and experimentally found values of resolution of our system.

Table- 1 Resolution of the system

Resolution	Seagar (Related to model)	Isaacson (Related to measurement precision)
Theoretically predicted	0.20	0.28
Experimentally established	0.23 @ center / 0.16 @periphery	0.23 @ center / 0.16 @periphery

3.2.3 Image quality parameters
As discussed before the quality of the image is assessed using Contrast to Noise Ratio (CNR) [4], Ringing (RNG) [8] and the actual reconstructed area.

In order to evaluate the CNR we have used cylindrical plastic pipes with different values of radius (2.1 to 1.5 cm). Data is acquired by placing outer edge of each pipe 1cm away from electrode 11. The reconstructed images are shown in Fig.10 along with the calculated value for CNR. The value of CNR ranges from 4.5 to 5.82 which is comparable, in fact better than that reported by Bera et al [4]

| CNR = 4.5 | CNR = 5.61 | CNR = 5.38 | CNR = 5.82 |
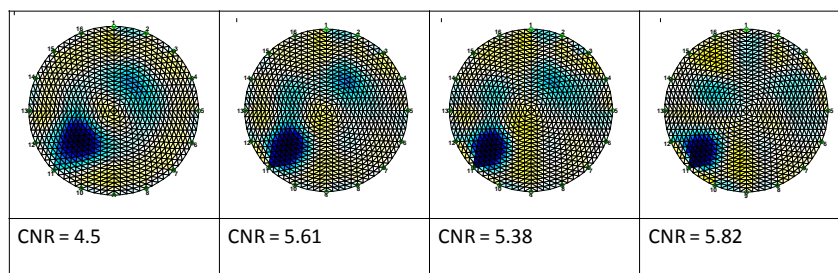
Figure 10. CNR for different images

To get an idea of Ringing (RNG) the reconstructed images for different currents with centrally placed plastic cylinder of radius 4.6 cm (Fig.3) are used. The calculated values for ringing are shown in Fig.11(b).

Reconstructed Area = 69.8 cm²
Actual Area = 66.48 cm²

Current (mA)	Ringing
0.6	4.78
0.7	4.55
0.8	4.42
0.9	4.37
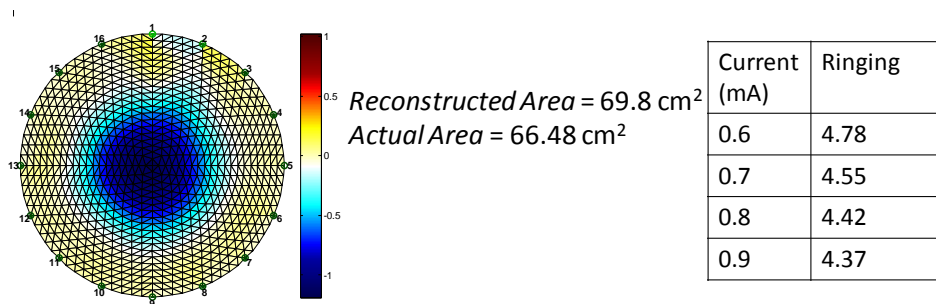
Figure 11. (a) Reconstructed area and (b) Ringing

We have used the same plastic cylinder of radius 4.6 cm placed at the center for obtaining the ratio of reconstructed target area and the actual area of target (Fig.11a). The plastic cylinder has cross sectional area equal to 66.48 cm². The reconstructed area of target is found as fraction of the total image area and is observed to be 0.2743. Vessel radius is 9 cm giving cross sectional area equal to 254.5 cm². Its fractional target area comes out to be 69.80 cm². Therefore the reconstructed target area matches well with the actual area.

IV. Conclusion

Performance of EIT system depends on the characteristics of its data and reconstructed image. We experimentally establish the effect of amplitude of injection current on image. It is found that the image is better when the current is set to give homogeneous data having peak value around 75% of the maximum allowed voltage as input to the DAQ. In different EIT systems there may be different variables under user's control. But if the parameter setting is done, such that the digitized signal has amplitude equal to 75% of maximum for plain homogeneous medium, then one can ensure good reconstructed images. This has been confirmed while collecting every data set in this work. The 16-electrode 2D EIT system developed in our laboratory is characterized for its performance. The SNR is found to be in the range 15 dB to 45 dB. The plot of SNR for all 208 channels uses the sequence proposed by Gagnon et al [17] and the plot takes the 'U' shape as expected. SNR is measured for two different conductivities and its value decreases for higher conductivity as expected. Accuracy is decided by comparing observed values with true value. The grid size for these simulations is chosen to give relative voltage errors well below 1% which is the variability of measuring system. Accuracy values are observed to be not uniform for all channels. The reason for this behavior needs to be explored. Resolution at the center is measured to be 0.23. It tallies well with the limit set by Isaacson's expression which uses system noise to decide the resolution. Such a comparison is done for the first time according to authors' knowledge. The resolution near the periphery is decided using PSF method and it is found to be better than that at the center. This fact agrees well with established fact that Sheffield pattern gives non uniform resolution. Image quality is decided using CNR and RNG. CNR is found to be in the range of 4.5 to 5.82 which are even better than some reported values. RNG is found to be in the range of 4.37 to 4.78. Reconstructed area for a centrally placed target matches the actual area of target with 4.7 % error. The guidelines for acquiring data are certainly important for getting improved images. Further work on exploring variation in the accuracy values for all channels and application of the system is being carried out.

References

[1]   Barber, D. C., and B. H. Brown. "Applied potential tomography." *Journal of Physics E: Scientific Instruments* 17.9 (1984): 723
[2]   Holder DS (ed). 2004 Electrical impedance tomography: methods, history and applications. Boca Raton, FL: CRC Press
[3]   Adler, Andy, and William RB Lionheart. "Uses and abuses of EIDORS: an extensible software base for EIT." *Physiological measurement* 27.5 (2006): S25
[4]   Bera, Tushar Kanti, and Jampana Nagaraju. "Resistivity imaging of a reconfigurable phantom with circular inhomogeneities in 2D-electrical impedance tomography." *Measurement* 44.3 (2011): 518-526
[5]   Yang, Chuan Li. *Electrical impedance tomography: algorithms and applications*. Diss. University of Bath, 2014
[6]   Sarode V, Patil H, Cheeran A, (2014) "LabVIEW based Automatic Data acquisition system for Electrical Impedance Tomography", International Journal of Computer Science and Information Technologies, Vol. 5 (3) , 2014, 4320-4324
[7]   Lionheart W (1990), "Image Reconstruction In Electrical Impedance Tomography", Ph.D. thesis University of Manchester
[8]   Maimaitijiang, Yasheng, et al. "A phantom based system to evaluate EIT performance." *Int. Conf. Electrical Bio-Impedance & Electrical Impedance Tomography Gainville, Fl, USA*. 2010
[9]   Ayati, S. Bentolhoda, et al. "Performance evaluation of a digital electrical impedance tomography system." (2012)
[10]   Ranade, Nanda V., and Damayanti C. Gharpure. "Design and development of instrumentation for acquiring electrical impedance tomography data." *Physics and Technology of Sensors (ISPTS), 2015 2nd International Symposium on*. IEEE, 2015

[11]   Isaacson, David. "Distinguishability of conductivities by electric current computed tomography." *IEEE transactions on medical imaging* 5.2 (1986): 91-95

[12]   Seagar, A. D., D. C. Barber, and B. H. Brown. "Theoretical limits to sensitivity and resolution in impedance imaging." *Clinical Physics and Physiological Measurement* 8.4A (1987): 13.

[13]   Bera, Tushar Kanti, and J. Nagaraju. "Studies on thin film based flexible gold electrode arrays for resistivity imaging in electrical impedance tomography." *Measurement* 47 (2014): 264-286

[14]   Chakraborty, Deborshi, Madhurima Chattopadhyay, and Radhaballabh Bhar. "Resistivity Imaging of a Phantom With Irregular Inhomogeneties With 16 Copper Electrodes Based Sensory System in 2 Dimensional Electrical Impedancer Tomography." *Proceeding. of International Conference on EEC*. 2013

[15]   Gaggero, Pascal Olivier, et al. "Electrical impedance tomography system based on active electrodes." *Physiological measurement* 33.5 (2012): 831

[16]   Song, Xiaomei, et al. "Automated region detection based on the contrast-to-noise ratio in near-infrared tomography." *Applied optics* 43.5 (2004): 1053-1062

[17]   Gagnon, Hervé, et al. "A resistive mesh phantom for assessing the performance of EIT systems." *IEEE transactions on biomedical engineering* 57.9 (2010): 2257-2266

[18]   Adler, Andy, and Robert Guardo. "Electrical impedance tomography: regularized imaging and contrast detection." *IEEE transactions on medical imaging* 15.2 (1996): 170-179

[19]   Adler, Andy, et al. "GREIT: a unified approach to 2D linear EIT reconstruction of lung images." *Physiological measurement* 30.6 (2009): S35

[20]   Wheeler, James L., Wei Wang, and Mengxing Tang. "A comparison of methods for measurement of spatial resolution in two-dimensional circular EIT images." *Physiological measurement* 23.1 (2002): 1